A multimodal treatment of carbon ions irradiation, miRNA-34 and mTOR inhibitor specifically control high-grade chondrosarcoma cancer stem cells

Guillaume Vares[a], *Vidhula Ahire*[b, c], *Shigeaki Sunada*[d,e], *Eun Ho Kim*[f], *Sei Sai*[g], *François Chevalier*[b, c], *Paul-Henri Romeo*[h], *Tadashi Yamamoto*[a], *Tetsuo Nakajima*[d] *and Yannick Saintigny*[b, c]

[a] Cell Signal Unit, Okinawa Institute of Science and Technology Graduate University (OIST), Tancha 1919-1, Onna-son, Okinawa, Japan
[b] Research Laboratory and Open Facility for Radiation Biology with Accelerated Ions (LARIA), CEA/DRF/IBFJ/IRCM, Campus Jules Horowitz, Boulevard Henri Becquerel, Caen, France
[c] Centre de Recherche sur les Ions, les Matériaux et la Photonique (CIMAP), Normandie Univ/ ENSICAEN/UNICAEN/CEA/CNRS, Campus Jules Horowitz, Boulevard Henri Becquerel, Caen, France
[d] Department of Radiation Effects Research, National Institutes for Quantum and Radiological Science and Technology (QST), Anagawa 4-9-1, Inage-ku, Chiba, Japan
[e] Department of Molecular Genetics, Tokyo Medical and Dental University (TMDU), 1-5-45 Yushima, Bunkyo-ku, Tokyo, Japan
[f] Division of Radiation Biomedical Research, Korea Institute of Radiological and Medical Sciences (KIRAMS), 75 Nowon-ro, Gongneung 2(i)-dong, Nowon-gu, Seoul, South Korea
[g] Department of Charged Particle Therapy Research, National Institutes for Quantum and Radiological Science and Technology (QST), Anagawa 4-9-1, Inage-ku, Chiba, Japan
[h] Research Laboratory on repair and Transcription in hematopoietic Stem Cells (LRTS), François Jacob Institute of biology, CEA/DRF/IBFJ/IRCM, 18 Route du Panorama, Fontenay-aux-Roses, France

Running title: *Efficient multimodal treatment of chondrosarcoma stem cells*

Corresponding authors

- Guillaume Vares, Cell Signal Unit, OIST, 1919-1 Tancha, Onna-son, Okinawa 904-0495, Japan. E-mail : guillaume.vares@oist.jp
- Yannick Saintigny, French Atomic Energy Commission, 18 Route du Panorama, BP6, Fontenay-aux-Roses 92265 CEDEX, France. E-mail: yannick.saintigny@cea.fr

Declarations of interest

None

Abbreviations

ALDH: aldehyde dehydrogenase; CFE: colony forming efficiency; CS: chondrosarcoma; CSC: cancer stem cell; LET: linear energy transfer; mTOR: mammalian target of rapamycin; NTCP: normal tissue complication probability; OER: oxygen enhancement ratio; PARP: poly ADP ribose polymerase; RBE: relative biological effectiveness; TCP: tumor control probability

New corresponding author address: Guillaume Vares, IRSN, PSE-SANTE/SESANE/LRTOX, B.P. 17, Fontenay-aux-Roses Cedex 92262, France. E-mail: guillaume.vares@irsn.fr
Accepted manuscript. Radiother Oncol. 2020 Jul 24;150:253-261. doi: 10.1016/j.radonc.2020.07.034.

Abstract

Background and purpose

High-grade chondrosarcomas are chemo- and radio-resistant cartilage-forming tumors of bone that often relapse and metastase. Thus, new therapeutic strategies are urgently needed.

Material and methods

Chondrosarcoma cells (CH-2879) were exposed to carbon-ion irradiation, combined with miR-34 mimic and/or rapamycin administration. The effects of treatment on cancer stem cells, stemness-associated phenotype, radioresistance and tumor-initiating properties were evaluated.

Results

We show that high-grade chondrosarcoma cells contain a population of radioresistant cancer stem cells that can be targeted by a combination of carbon-ion therapy, miR-34 mimic administration and/or rapamycin treatment that triggers FOXO3 and miR-34 over-expression. mTOR inhibition by rapamycin triggered FOXO3 and miR-34, leading to KLF4 repression.

Conclusion

Our results show that particle therapy combined with molecular treatments effectively controls cancer stem cells and may overcome treatment resistance of high-grade chondrosarcoma.

Keywords

cancer stem cell, chondrosarcoma, particle therapy, mTOR inhibitor, miR-34

1. Introduction

Despite striking improvements in the diagnosis and care of human cancer, treatment resistance remains to this day an issue in some hard-to-treat cancers. Chondrosarcomas (CSs) constitute the second most common primary bone tumor in adults [1]. Because these cartilaginous tumors exhibit resistance to chemotherapy and conventional radiation therapy, complete surgical resection still remains the primary treatment, with a 10-year survival rate comprised between 30% and 80% depending on the grade. A significant number of patients experience relapse, metastasis or present unresectable disease with poor clinical outcome and high lethality (grade III). For those reasons, the clinical management of CS is considered to be particularly challenging, and new therapeutic approaches are urgently needed. Some subtypes, such as mesenchymal CS, may be more responsive to chemotherapy, while surgery of dedifferentiated CS may be more successful when combined with chemotherapy [2]. Radiation therapy has been used in skull-base and spinal CS [3,4]. Recently published molecular therapy targets for CS have included IDH mutations, Hedgehog, Src and PI3K-Akt-mTOR pathways, histone deacetylase inhibitors, angiogenesis or immunotherapy with immune checkpoint inhibition [5]. Some of those targets yielded promising results in preclinical studies, but early phase clinical results were less conclusive.

Cancer stem cells (CSCs) are defined as the subset of dedifferentiated cells within a tumor that possess the ability to self-renew and reconstitute tumor heterogeneity[6]. CSCs are more resistant than their non-CSC counterparts and were suggested to be at least partially responsible for treatment resistance, relapse and metastasis[7]. Cancer treatments that do not effectively target CSCs might ultimately fail, thus it is of paramount importance to develop new treatment strategies that include CSCs. Transformed mesenchymal stem and progenitor cells with multipotent differentiation potential are likely to be cells of origin in CS [8]. CSCs have been characterized in osteosarcomas [9], but are not well defined in CS.

New high linear energy transfer (LET) radiation therapy modalities (such as heavy-ion particle beams) have emerged, which provide a number of physical and biological advantages over conventional X-ray therapy (including an improved relative biological effectiveness RBE and a lower oxygen enhancement ratio OER) and might finally contribute to overcoming treatment resistance [10]. High LET radiation treatment, in combination with other therapies (for example, the chemotherapeutic agent cisplatin or the PARP inhibitor talazoparib), has shown favourable results in bypassing tumor and CSC radioresistance [11–15]. Although we have recently shown that low- and high-LET low-dose exposures of CS cells can trigger bystander responses in non-irradiated neighbouring normal chondrocytes [16], the high RBE of carbon ions might allow lower normal tissue complication probability (NTCP) than protons, for the same local tumor control (TCP) [17], indicating that carbon ion therapy might be an appropriate CS treatment modality. In this study, we investigated the ability of high LET radiation combined with targeted treatments to target CS cells and CSCs.

2. Material and methods

Cell culture, treatment and sorting of cancer stem cells. CH-2879 chondrosarcoma cells [18] were authenticated by Short Tandem Repeat (STR) profiling. Cells were grown in RPMI1640 medium (Nacalai, Kyoto, Japan) supplemented with 10% fetal bovine serum (FBS) (Cosmo Bio, Tokyo, Japan) and antibiotic-antimycotic solution (Penicillin, Streptomycin, Amphotericin B. Gibco ThermoFisher, Carlsbad, CA, USA). Cultures were grown in 5% CO_2 at 95% humidity. Cells were treated for 48h with rapamycin at a final concentration of 1 nM. Cells were transfected with miRCURY LNA miR-34a Mimic (Qiagen, Hilden, Germany) using Lipofectamine RNAiMax reagent (Invitrogen), according to the manufacturer's instructions, at a final concentration of 5 nM. Cells not transfected with the mimic were treated with lipofectamine alone. ALDH activity in the cells was measured by flow cytometry using the ALDEFLUOR kit (Stemcell technologies, Vancouver, BC, Canada) as previously [19]. Cells with low and high levels of ALDH enzymatic activity (respectively $ALDH^-$ and $ALDH^+$ cells) were sorted using a FACSAria cell sorter (BD Biosciences, Franklin Lakes, NJ, USA).

As a negative control, cells were treated with diethylaminobenzaldehyde (DEAB), a specific ALDH inhibitor.

Radiation exposure. X-ray irradiations were conducted using an M-150WE X-ray generator (Softex, Tokyo, Japan) at 140 kVp, 8 mA, 80V. Irradiation dose-rate was 1.3 Gy/min. Particle therapy experiments were performed at the Heavy Ion Medical Accelerator in Chiba (HIMAC). Cells were irradiated with a 290 MeV/n carbon-ion beam at the center of a 6 cm Spread-Out Bragg Peak (SOBP) as previously [11].

Sphere formation assay. Cells were seeded in triplicate in ultra-low attachment plates (Corning, Corning, NY, USA) with serum-free culture medium at defined densities and grown for 10 days. Spheres larger than 60 μm in size were counted.

Colony Forming Efficiency (CFE) assay. After irradiation, cells were seeded at defined densities and incubated for 10–14 days then stained. Colonies with more than 50 cells were scored and surviving fractions were determined after correcting for the plating efficiency as previously described [20]. Survival curve data were fitted to the linear (carbon-ion) or linear-quadratic model (X-rays) and are presented as the mean of at least three independent experiments.

Invasion scratch assay. Cells were seeded in triplicate in 24-well plates. 16 hours before assays, culture medium was replaced with serum-free medium, then a wound was introduced into the confluent monolayer with a pipette tip. Percentage of wound closure 24 hours later was measured with ImageJ software.

Oxidative stress quantification. Intracellular levels of reactive oxygen species (ROS) were measured using 5-(and-6)-chloromethyl-29,79-dichloro- dihydrofluorescein diacetate, acetyl ester (CM-H2DCFDA, Molecular Probes, Eugene, OR, USA). Cells were plated in 6-well plates, then 24 hours later 10 mM CM-H2DCFDA was added and cells were incubated for 40 minutes. Fluorescence

intensities were measured using a SpectraMax M5 microplate reader (Molecular Devices, Sunnyvale, CA, USA) (excitation at 493 nm, emission at 520 nm). Unstained cells were used as negative control. Results are presented as the mean of three independent experiments.

Real-time PCR gene expression profiling. RNA was extracted using TRIzol reagent and PureLink RNA Mini Kit (ThermoFisher). cDNA was synthesized using the PrimeScript RT kit (Takara Bio, Kusatsu, Japan) for mRNAs or the Mir-X First-Strand Synthesis Kit (Takara Bio) for microRNAs. Then quantitative real-time polymerase chain reaction (qRT-PCR) was run in triplicate in 384-well plates, using SYBR Premix Ex Taq II (for mRNAs, Takara Bio) or TB Green Advantage qPCR Premix (for microRNAs, Takara Bio), on a ViiA 7 real-time PCR system (ThermoFisher). Relative mRNA levels were calculated using the ΔΔCt method and normalized to GAPDH (for mRNAs) or U6 (for microRNAs).

Western blotting. CH-8279 cells were lysed with radioimmunoprecipitation assay (RIPA) buffer (Santa Cruz Biotechnology, Dallas, TX, USA). Protein concentrations were determined using the Protein Assay CBB solution (Nacalai) using bovine serum albumin (BSA) as a standard. Protein expression levels were measured using a Wes Simple Western instrument (ProteinSimple, San Jose, CA, USA), with KLF4 (Cell Signaling Technologies, Danvers, MA, USA, #4038S) and GAPDH (Cell Signaling #2118L) antibodies, according to the manufacturer's instructions [21]. Raw electropherograms were used to generate blot-like images.

Reporter assays. CH-2879 cells were transfected using Lipofectamine 3000 reagent with pGL3-FOXO3-Luciferase reporter, pRL-TK control reporter and/or pCMV-FOXO3 expression vector. Firefly and Renilla luciferase activities were measured using the Dual Luciferase Assay System (Promega, Madison, WI, USA). Normalized luciferase activities were obtained as previously.

Mouse experiments. 4-week old BALB/c nu/nu male mice (Japan SLC, Hamamatsu, Japan) were distributed 3 animals to a cage and maintained on a 12-hr light/12-hr dark cycle in a temperature-controlled (22°C) barrier facility with free access to water and a normal diet (CLEA Japan, Tokyo, Japan). Mice were allowed to acclimatize for 5 days before the experiment. Variable numbers of ALDH- and ALDH+ chondrosarcoma cells mixed 1:1 with Matrigel Growth Factor Reduced (Corning, Corning, NY, USA) were injected subcutaneously into mouse flank on both sides under isoflurane anesthesia. 4 to 9 mice were used per experimental group (for a total of 31 mice). Five days later, miRCURY LNA miR-34 Mimic (Qiagen) was injected on one side with MaxSuppressor in vivo RNALancer II delivery system (Bioo Scientific, Austin, TX, SA), according to manufacturer instructions; 25 µL of mimic/phospholipid-oil emulsion diluted in PBS were injected (1 nmol total miRNA mimic). On the other side, phospholipid-oil emulsion without mimic was injected. Tumor volumes were measured using calipers [22]. After experiments, mice were euthanized by carbon dioxide inhalation. Mouse experiment protocols were approved by the Animal Care and Use Committee at Okinawa Institute of Science and Technology Graduate University.

Statistical analysis. Clonogenic survival curve data were fitted to the linear-quadratic model (for X-ray irradiations) or linear model (for carbon-ion irradiation), using the CS-Cal software (www.oncoexpress.de), as previously [23]. Statistical significance of the difference between dose-response curves was performed using one-sided 2-class t-test, Welsh and Sattlewaith approximation for each dose, with SigmaPlot software (systatsoftware.com/products/sigmaplot/) (* P<0.05). Other significant differences were assessed using Student's t-test (* P<0.05). Errors bars represent standard deviation.

3. Results

Subpopulations of cancer stem cells (CSCs) have been identified in sarcomas [24]. Among a panel of four chondrosarcoma cell lines (CH-2879, OUMS27, L835, SW-1353) (Table A1), CH-2879 cells

and, to a lesser extent, OUMS27 cells, could grow as spheres, indicating that they may contain CSCs [25,26]. The CH-2879 cell line was established from a recurrent Grade III chondrosarcoma of the chest wall [18], with tumorigenic and invasive abilities. Because CSCs have been associated with tumorigenicity and metastasis, CH-2879 may be a good model to study treatment responses of grade III chondrosarcomas.

We and others have previously shown that aldehyde dehydrogenase (ALDH) activity is a useful marker for CSC-like populations in various cancer models [19]. Here, CH-2879 cells contained an $ALDH^+$ subpopulation (around 1%) that exhibited increased sphere formation and invasion abilities associated with a low level of reactive oxygen species (ROS) (Figure 1abcd). Exposure of CH-2879 cells to carbon-ion beam resulted in significant cell death and the induction of stress response pathways (Figure A1). We then compared clonogenic survival of $ALDH^-$ and $ALDH^+$ cells after exposure to X-rays and carbon-ion beam (Figure 1e). As expected, particle therapy had a higher relative biological efficiency (RBE) and $ALDH^+$ cells were markedly more radioresistant to X-rays and carbon-ion beam (Table 1). However, relative biological efficiencies (RBEs) for $ALDH^-$ and $ALDH^+$ cells were similar, suggesting that particle therapy alone was not sufficient to target CSCs in CS.

miR-34 is a tumor-suppressive micro-RNA associated with the regulation of stem-like cells in prostate cancer, pancreatic cancer or glioblastoma [28–30]. Administration of a synthetic miR-34 mimic decreased sphere formation and invasion capabilities of CH-2879 ALDH+ cells (Figure 1bc), and increased ROS levels (Figure 1d), indicating that the maintenance of chondrosarcoma stem-like phenotype may rely also on miR-34 repression. Indeed, miR-34 expression levels were lower in ALDH+ cells than in ALDH- cells (Figure 2a)

The effect of miR-34 mimic did not rely on the selective elimination of CSCs via apoptosis (Figure A2), but rather on the disturbance of the dynamic equilibrium between CSCs and non-CSCs. Expression of miR-34 target genes [31] *NOTCH1*, *C-MYC*, *LMTK3* and *KLF4* were repressed in

response to miR-34 mimic treatment (Figure 2b), resulting in lower proportion of ALDH+ cells (Figure 1a). KLF4 protein expression was detected in ALDH+ cells, but not in ALDH- cells or ALDH+ cells treated with miR-34 mimic (Figures 2c, A3). As observed in breast cancer [19], KLF4 seems to play a role in CSC maintenance in CS, since treatment with *KLF4* siRNA partially recapitulated the effects of miR-34 mimic (Figure 2d).

CH-2978 cells were able to generate tumor xenografts in nude mice (Figure 2e). Tumors were observed when as few as 10,000 $ALDH^+$ cells were injected (with 100% of the mice developing tumors), whereas $ALDH^-$ cells had very low tumor initiation potential. Administration of miR-34 mimic together with tumor cells resulted in a significant decrease in tumor formation, with less than half of mice developing tumors after injection of 100,000 ALDH+ cells (Table 2). However, when miR-34 mimic was delivered one month after xenograft, it couldn't shrink tumors and could only slow down tumor growth (Figure 2f). This suggested that miR-34 treatment alone may not be sufficient in established tumors (or that mimic delivery efficiency needs to be improved) and that combination therapies might be necessary.

The PI3K-Akt-mTOR pathway has recently emerged as a promising target for intervention in chondrosarcoma [32–35]. Compelling evidence also indicates an important role of mTOR pathway in CSC maintenance. Rapamycin, an mTORC1 inhibitor, inhibited the proliferation of CH-2879 cells (Figure A4). Although rapamycin had a slight radio-sensitizing effect (Figure A5), it decreased the proportion of ALDH+ CSCs (Figure 1a). Interestingly, rapamycin administration led to slightly increased levels of miR-34 (Figure 3a) and lower miR-34 target gene levels (*NOTCH1*, *C-MYC*, *LMTK3*, *KLF4* and *Rictor*), with a significant repression of *KLF4* expression (Figure 3b).

Forkhead box O (FOXO) transcription factors are crucial regulators of cell signaling, and coordinate Akt and mTOR activities [36]. Over-expression of FOXO3 enhanced FOXO3 promoter activity (Figure 3c) and was associated with $ALDH^+$ cells losing sphere forming abilities (Figure 3d).

Finally, FOXO3 over-expression resulted in higher miR-34 expression levels (Figure 3e) and lower levels of miR-34 target genes, including KLF4 transcript (Figure 3f) and protein (Figure 2c). The effect of Rapamycin on CSCs was counteracted when using an siRNA for FOXO3 (Figures 1 and 3d). Altogether, these results suggest that rapamycin effects in chondrosarcoma rely on FOXO3 activity.

Combined action of rapamycin and miR-34 mimic led to sustained inhibition of sphere-forming abilities of CH-2879 cells, compared to individual treatments (Figure 4a). Using combined treatment, it was possible to effectively control CSC subpopulations after exposure to carbon-ion doses as low as 1 Gy, as the resulting cell populations contained at least 10 times less CSCs than non-treated population (Figure 4b). Such control was not observed when cells were exposed with a roughly equivalent X-ray dose of 2 Gy, based on an RBE of ~1.9 (Table 1). By altering CSC-like phenotype, rapamycin and miR-34 mimic treatments (alone or combined) prompted the radio-sensitization of ALDH+ cells. Although the overall effect of those treatments on the global radio-sensitivity is limited (Figure A5), the near-complete elimination of CSC-like phenotype after combination treatments may effectively address CSC-associated treatment resistance.

4. Discussion

Surgical resection constitutes the cornerstone of treatment for chondrosarcoma (CS), as chemotherapy is most often ineffective. Histologic grade is considered to be the most important indicator of prognosis, and the outcome for grade III CS with surgical resection alone is usually relatively poor [37]. CH-2879, a cell line isolated from recurrent grade III CS, was selected as a suitable model for the development of new therapeutic strategies in hard-to-treat CSs.

Cancer stem cells (CSCs) have long been presented as an important culprit for treatment resistance [38]. Indeed, different tumors harbor various CSC contents, and the proportion of CSCs may be correlated with radio-resistance [39]. Stem-like properties of CSCs confer them a survival advantage during cancer therapy. Those include higher reactive-oxygen species (ROS) scavenging abilities

(resulting in lower radiation-induced ROS) and improved DNA damage repair activation [40]. It is therefore of outmost importance to properly identify and target the stem-like population when establishing new treatment regimen. In CS, a subpopulation of CD133+ cells have been identified that display stem-like characteristics and were capable of inducing and sustain tumor growth *in vivo* [24]. Significant evidence indicates that enhanced aldehyde dehydrogenase (ALDH) activity is a hallmark of CSCs and is directly involved in CSC-associated resistance [41]. ALDH+ breast cancer cells exhibit increased DNA repair abilities and higher survival in response to radiation exposure, associated with the stimulation of Nanog, BM1, Notch1 and Akt [42]. For these reasons, identification of ALDH+ cells is generally considered to be a reliable marker for stem-like subpopulations [43]. Moreover, the identification of ALDH as a key player in resistance to radiation therapy and tumor recurrence suggest that ALDH may be considered as a potential therapeutic target [44]. Here, sorted ALDH+ CH-2879 cells exhibited a number of CSC distinctive features, such as lower ROS levels, increased self-renewing abilities (as indicated by sphere formation assay), enhanced invasiveness, radioresistance and in *vivo* tumorigenicity. This suggested that in addition to CD133, ALDH expression should also be an appropriate marker for the identification of stem-like radioresistant subpopulations in CS.

The relative biological efficiency (RBE) of the spread-out Bragg peak (SOBP) carbon-ion beam at the Heavy Ion Medical Accelerator in Chiba (HIMAC), relative to conventional X-rays, was within the previously observed range (1.5-2.5) in other experimental models [11–13]. It was lower than the RBE of the monoenergetic carbon-ion beam at the Grand Accélérateur National d'Ions Lourds (GANIL) [16]. Although ALDH+ cells were more radioresistant than ALDH- cells, their respective RBEs (whether at D10 or at D37) were not significantly different. While carbon-ion beam alone may be more efficient against CSCs in some models [45,46], these results demonstrated that the treatment of CS should not rely solely on particle therapy and therefore combination treatments may be needed.

The relationship between CSCs and non-stem cancer cells (NSCCs) has been a matter of enormous attention. CSCs and NSCCs coexist in a highly dynamic, bidirectional equilibrium state, whose maintenance is under the control of a not fully understood molecular crosstalk between CSCs, NSCCs and the tumor microenvironment [47]. microRNAs closely regulate pluripotency and differentiation mechanisms, and a number of CSC-associated microRNA regulations have been described [48]. miR-34 is a well-known tumor-suppressor transcriptionally activated by p53, which has been associated with cancer stem cell homeostasis in several experimental models [29,30,49]. mir-34 expression is downregulated in chondrosarcoma cell lines, compared to primary non-tumorous articular chondrocytes [50]. Here, we show that in CH-2879 CS cell line, administration of a miR-34 mimic was capable of decreasing stem-like radioresistant subpopulations.

Hundreds of direct miR-34 targets have been identified, with an over-representation of mRNAs involved in cell cycle control, DNA damage response and apoptosis [51]. Notch homolog 1 (NOTCH1), C-MYC, Lemur Tyrosine Kinase 3 (LMTK3) and Krüppel-like factor 4 (KLF4) have all been identified as having a role in maintenance of self-renewal, chemoresistance, invasion and/or stem-like properties in cancer [52–55]. KLF4, one of the so-called Yamanaka pluripotency factors, was described either as a tumor-suppressor or as an oncogene, depending on the cancer type [56]. In osteosarcoma, KLF4 enhances proliferation and metastasis via alpha-crystallin B chain (CRYAB) [57]. In breast cancer, expression of KLF4 is determinant for the maintenance of CSCs [19,58] and KLF4 seems to play a similar role in CS. Because KLF4 siRNA only partially recapitulated the effect of miR-34 on CSC-like phenotype, we can hypothesize that while KLF4 is a probably a major effector of miR-34 in CSCs, other pathways regulated by miR-34 are expected to be involved. As a matter of fact, miR-34 is able to suppress stem-like characteristics in breast cancer by downregulating Notch pathway [59]. Furthermore, ALDH mRNA levels are reduced in tumor tissues of miR-34-treated mice [60]. Because ALDHs are involved in ROS scavenging [41,61], miR-34 effects might rely on ROS accumulation, leading to increased radiosensitivity. Although miR-34 expression levels may not be directly correlated

with survival in TCGA data of sarcoma patients, low expression of several miR-34 target genes (C-MYC, Cyclin-dependent kinase 4 – CDK4, Cyclin-dependent kinase 6 – CDK6, E2F Transcription Factor 3 – E2F3) is associated with better sarcoma survival (Table A3, Figure A6). miR-34 therapy may be effective mainly as a combination with other treatment modalities.

Mammalian target of rapamycin (mTOR) is a Ser/Thr kinase that is regulated in an extensive list of functions, including proliferation, survival, cytoskeleton organization or metabolism. mTOR is the catalytic subunit of two functionally distinct protein complexes: mTOR complex 1 (mTORC1) and mTORC2. The aberrant activation of mTOR activity is observed in multiple cancer types, resulting from phosphoinositide 3-kinase (PI3K) amplification/mutation, phosphatase and tensin homolog (PTEN) loss of function, or from the overexpression of Akt, Ribosomal protein S6 kinase beta-1 (S6K1), eukaryotic translation initiation factor 4E-binding protein 1 (eIF4EBP1) or eIF4E. For this reason, mTOR pathway inhibition is regarded as an important target for the development of new cancer therapies. Phosphorylation of S6K1 was detected in 69% of conventional CS and 44% of dedifferentiated CS [32], suggesting that mTOR inhibition may be a good strategy for CS therapy.

Surprisingly, inhibition of mTORC1 by rapamycin lowered the proportion of CSCs. The role of S6K1 and eIF4eBP1 in mTORC1-mediated regulation of translation is well known. Moreover, forkhead box O (FOXO) transcription factors are crucial regulators of cellular homeostasis and are known tumor suppressors in human cancers [62]. The complex interplay between FOXO, mTOR and Akt has been described [36]. FOXOs decrease ROS levels and inhibit mTORC1 via Sestrin3 [63]. On the other hand, it was also reported that the mTOR pathway is capable of regulating FOXO3 activity by downregulating glucocorticoid-inducible kinase 1 (SGK1), which is responsible for FOXO3 phosphorylation. The inactivation of mTORC1 induced by p18 depletion led to FOXO3 hypophosphorylation at Ser314 [64]. Here, we show that inhibition of mTORC1 led to increased FOXO3 promoter activity and that it directly led to the reversal of CSC-like phenotype. FOXO3 is a

323 transcriptional regulator of miR-34 [65,66] and its activation led to the inhibition of miR-34 targets
324 like KLF4.

325 Therefore, inactivation of mTORC1 by rapamycin has direct effects on miR-34-associated
326 pathways. Rapamycin treatment together with miR-34 mimic administration had a sustain inhibitory
327 effect on CSC-like phenotype. However, the fact that the combination of miR-34 mimic and rapamycin
328 administration is more potent than rapamycin alone suggests that alternative molecular mechanisms
329 are also likely to be involved. In non-treated cells, only higher irradiation doses led to significant
330 effects (such as the induction of cell death pathways). However, high dose exposures can lead to a
331 relative CSC enrichment [67,68]. By delivering a combination treatment, it was then possible to further
332 decrease irradiation doses while efficiently suppressing CSC-like attributes.

333 Altogether, these results suggest that mTOR inhibition by rapamycin supplemented with miR-34
334 mimic treatment may be able to overcome CSC-associated radioresistance in chondrosarcoma during
335 carbon-ion therapy. Combination treatments might also improve the effectiveness of carbon-ion
336 therapies at lower doses, decrease risks of relapse and metastasis, and better preserve surrounding
337 normal tissues against non-targeted effects.

Acknowledgments

The authors would like to thank Charlotte Lepleux (CIMAP) and Mihaela Temelie (NIPNE) for scientific and technical help. This work was carried out as a part of Research project with Heavy ion at HIMAC (Project #15J104). This work was supported by the Transverse Division n°4 (Radiobiology) of the French Alternative Energies and Atomic Energy Commission; Okinawa Institute of Science and Technology Graduate University (OIST); JSPS-MAEDI France-Japan Bilateral Joint Research Program "Sakura" (PHC 35973SB, JSPS 16031011-000323); ANR (Equipex Rec-Hadron ANR-10-EQPX-1401 and Investissement d'Avenir France Hadron 11-INBS-0007); Ligue contre le Cancer, comités de Normandie (comité de l'Orne); JSPS Kakenhi Grant-in-Aid for Scientific Research (19K07765).

References

[1]Leddy LR, Holmes RE. Chondrosarcoma of Bone. In: Peabody TD, Attar S, editors. Orthopaedic Oncology: Primary and Metastatic Tumors of the Skeletal System, Cham: Springer International Publishing; 2014, p. 117–30. https://doi.org/10.1007/978-3-319-07323-1_6.

[2]van Maldegem AM, Bovée JV, Gelderblom H. Comprehensive analysis of published studies involving systemic treatment for chondrosarcoma of bone between 2000 and 2013. Clin Sarcoma Res 2014;4:11. https://doi.org/10.1186/2045-3329-4-11.

[3]Gatfield ER, Noble DJ, Barnett GC, Early NY, Hoole ACF, Kirkby NF, et al. Tumour Volume and Dose Influence Outcome after Surgery and High-dose Photon Radiotherapy for Chordoma and Chondrosarcoma of the Skull Base and Spine. Clinical Oncology 2018;30:243–53. https://doi.org/10.1016/j.clon.2018.01.002.

[4]Sanusi O, Arnaout O, Rahme RJ, Horbinski C, Chandler JP. Surgical Resection and Adjuvant Radiation Therapy in the Treatment of Skull Base Chordomas. World Neurosurgery 2018;115:e13–21. https://doi.org/10.1016/j.wneu.2018.02.127.

[5]Polychronidou G, Karavasilis V, Pollack SM, Huang PH, Lee A, Jones RL. Novel therapeutic approaches in chondrosarcoma. Future Oncology 2017;13:637–48. https://doi.org/10.2217/fon-2016-0226.

[6]Prager BC, Xie Q, Bao S, Rich JN. Cancer Stem Cells: The Architects of the Tumor Ecosystem. Cell Stem Cell 2019;24:41–53. https://doi.org/10.1016/j.stem.2018.12.009.

[7]Schulz A, Meyer F, Dubrovska A, Borgmann K. Cancer Stem Cells and Radioresistance: DNA Repair and Beyond. Cancers 2019;11:862. https://doi.org/10.3390/cancers11060862.

[8]Boehme KA, Schleicher SB, Traub F, Rolauffs B. Chondrosarcoma: A Rare Misfortune in Aging Human Cartilage? The Role of Stem and Progenitor Cells in Proliferation, Malignant Degeneration and Therapeutic Resistance. International Journal of Molecular Sciences 2018;19:311. https://doi.org/10.3390/ijms19010311.

[9]Heymann D, Brown HK, Tellez-Gabriel M. Cancer Stem Cells in Osteosarcoma. Cancer Letters 2017;386:189–95.

[10]Loeffler JS, Durante M. Charged particle therapy—optimization, challenges and future directions. Nature Reviews Clinical Oncology 2013;10:411–24. https://doi.org/10.1038/nrclinonc.2013.79.

[11]Sai S, Suzuki M, Kim EH, Hayashi M, Vares G, Yamamoto N, et al. Effects of carbon ion beam alone or in combination with cisplatin on malignant mesothelioma cells in vitro. Oncotarget 2017;9:14849–61. https://doi.org/10.18632/oncotarget.23756.
[12]Sai S, Vares G, Kim EH, Karasawa K, Wang B, Nenoi M, et al. Carbon ion beam combined with cisplatin effectively disrupts triple negative breast cancer stem-like cells in vitro. Molecular Cancer 2015;14:166. https://doi.org/10.1186/s12943-015-0429-7.
[13]Sai S, Wakai T, Vares G, Yamada S, Kamijo T, Kamada T, et al. Combination of carbon ion beam and gemcitabine causes irreparable DNA damage and death of radioresistant pancreatic cancer stem-like cells in vitro and in vivo. Oncotarget 2015;6:5517–35.
[14]Bertrand G, Maalouf M, Boivin A, Battiston-Montagne P, Beuve M, Levy A, et al. Targeting Head and Neck Cancer Stem Cells to Overcome Resistance to Photon and Carbon Ion Radiation. Stem Cell Rev and Rep 2014;10:114–26. https://doi.org/10.1007/s12015-013-9467-y.
[15]Lesueur P, Chevalier F, El-Habr EA, Junier M-P, Chneiweiss H, Castera L, et al. Radiosensitization Effect of Talazoparib, a Parp Inhibitor, on Glioblastoma Stem Cells Exposed to Low and High Linear Energy Transfer Radiation. Scientific Reports 2018;8:3664. https://doi.org/10.1038/s41598-018-22022-4.
[16]Lepleux C, Marie-Brasset A, Temelie M, Boulanger M, Brotin É, Goldring MB, et al. Bystander effectors of chondrosarcoma cells irradiated at different LET impair proliferation of chondrocytes. J Cell Commun Signal 2019. https://doi.org/10.1007/s12079-019-00515-9.
[17]Durante M, Orecchia R, Loeffler JS. Charged-particle therapy in cancer: clinical uses and future perspectives. Nature Reviews Clinical Oncology 2017;14:483–95. https://doi.org/10.1038/nrclinonc.2017.30.
[18]Gil-Benso R, Lopez-Gines C, Lopez-Guerrero JA, Carda C, Callaghan RC, Navarro S, et al. Establishment and characterization of a continuous human chondrosarcoma cell line, ch-2879: comparative histologic and genetic studies with its tumor of origin. Lab Invest 2003;83:877–87.
[19]Vares G, Sai S, Wang B, Fujimori A, Nenoi M, Nakajima T. Progesterone generates cancer stem cells through membrane progesterone receptor-triggered signaling in basal-like human mammary cells. Cancer Letters 2015;362:167–73. https://doi.org/10.1016/j.canlet.2015.03.030.
[20]Franken NA, Rodermond HM, Stap J, Haveman J, van Bree C. Clonogenic assay of cells in vitro. Nat Protoc 2006;1:2315–9. https://doi.org/10.1038/nprot.2006.339.
[21]Harris VM. Protein Detection by Simple Western™ Analysis. In: Kurien BT, Scofield RH, editors. Western Blotting: Methods and Protocols, New York, NY: Springer New York; 2015, p. 465–8. https://doi.org/10.1007/978-1-4939-2694-7_47.
[22]Tomayko MM, Reynolds CP. Determination of subcutaneous tumor size in athymic (nude) mice. Cancer Chemother Pharmacol 1989;24:148–54. https://doi.org/10.1007/bf00300234.
[23]Vares G, Wang B, Ishii-Ohba H, Nenoi M, Nakajima T. Diet-Induced Obesity Modulates Epigenetic Responses to Ionizing Radiation in Mice. PLOS ONE 2014;9:e106277. https://doi.org/10.1371/journal.pone.0106277.
[24]Tirino V, Desiderio V, Paino F, De Rosa A, Papaccio F, Fazioli F, et al. Human primary bone sarcomas contain CD133+ cancer stem cells displaying high tumorigenicity in vivo. The FASEB Journal 2011;25:2022–30. https://doi.org/10.1096/fj.10-179036.
[25]Fujiwara T, Ozaki T. Overcoming Therapeutic Resistance of Bone Sarcomas: Overview of the Molecular Mechanisms and Therapeutic Targets for Bone Sarcoma Stem Cells. Stem Cells Int 2016;2016. https://doi.org/10.1155/2016/2603092.
[26]Gibbs CP, Kukekov VG, Reith JD, Tchigrinova O, Suslov ON, Scott EW, et al. Stem-Like Cells in Bone Sarcomas: Implications for Tumorigenesis. Neoplasia 2005;7:967–76.
[27]Lee C-H, Yu C-C, Wang B-Y, Chang W-W. Tumorsphere as an effective in vitro platform for screening anti-cancer stem cell drugs. Oncotarget 2015;7:1215–26.
[28]Guessous F, Zhang Y, Kofman A, Catania A, Li Y, Schiff D, et al. microRNA-34a is tumor suppressive in brain tumors and glioma stem cells. Cell Cycle 2010;9:1031–6. https://doi.org/10.4161/cc.9.6.10987.
[29]Liu C, Kelnar K, Liu B, Chen X, Calhoun-Davis T, Li H, et al. The microRNA miR-34a inhibits prostate cancer stem cells and metastasis by directly repressing CD44. Nat Med 2011;17:211–5. https://doi.org/10.1038/nm.2284.

[30] Nalls D, Tang SN, Rodova M, Srivastava RK, Shankar S. Targeting epigenetic regulation of miR-34a for treatment of pancreatic cancer by inhibition of pancreatic cancer stem cells. PLoS One 2011;6:e24099. https://doi.org/10.1371/journal.pone.0024099.
[31] Misso G, Di Martino MT, De Rosa G, Farooqi AA, Lombardi A, Campani V, et al. Mir-34: a new weapon against cancer? Mol Ther Nucleic Acids 2014;3:e194. https://doi.org/10.1038/mtna.2014.47.
[32] Zhang Y-X, Oosterwijk JG van, Sicinska E, Moss S, Remillard SP, Wezel T van, et al. Functional Profiling of Receptor Tyrosine Kinases and Downstream Signaling in Human Chondrosarcomas Identifies Pathways for Rational Targeted Therapy. Clin Cancer Res 2013. https://doi.org/10.1158/1078-0432.CCR-12-3647.
[33] Perez J, Decouvelaere AV, Pointecouteau T, Pissaloux D, Michot JP, Besse A, et al. Inhibition of Chondrosarcoma Growth by mTOR Inhibitor in an In Vivo Syngeneic Rat Model. PLOS ONE 2012;7:e32458. https://doi.org/10.1371/journal.pone.0032458.
[34] Bernstein-Molho R, Kollender Y, Issakov J, Bickels J, Dadia S, Flusser G, et al. Clinical activity of mTOR inhibition in combination with cyclophosphamide in the treatment of recurrent unresectable chondrosarcomas. Cancer Chemother Pharmacol 2012;70:855–60. https://doi.org/10.1007/s00280-012-1968-x.
[35] Thornton KA, Chen AR, Trucco MM, Shah P, Wilky BA, Gul N, et al. A dose-finding study of temsirolimus and liposomal doxorubicin for patients with recurrent and refractory bone and soft tissue sarcoma. Int J Cancer 2013;133:997–1005. https://doi.org/10.1002/ijc.28083.
[36] Hay N. Interplay between FOXO, TOR, and Akt. Biochimica et Biophysica Acta (BBA) - Molecular Cell Research 2011;1813:1965–70. https://doi.org/10.1016/j.bbamcr.2011.03.013.
[37] Fiorenza F, Abudu A, Grimer RJ, Carter SR, Tillman RM, Ayoub K, et al. Risk factors for survival and local control in chondrosarcoma of bone. J Bone Joint Surg Br 2002;84:93–9.
[38] Eyler CE, Rich JN. Survival of the Fittest: Cancer Stem Cells in Therapeutic Resistance and Angiogenesis. J Clin Oncol 2008;26:2839–45. https://doi.org/10.1200/JCO.2007.15.1829.
[39] Baumann M, Krause M, Hill R. Exploring the role of cancer stem cells in radioresistance. Nat Rev Cancer 2008;8:545–54. https://doi.org/10.1038/nrc2419.
[40] Rich JN. Cancer Stem Cells in Radiation Resistance. Cancer Res 2007;67:8980–4. https://doi.org/10.1158/0008-5472.CAN-07-0895.
[41] Vassalli G. Aldehyde Dehydrogenases: Not Just Markers, but Functional Regulators of Stem Cells. Stem Cells Int 2019;2019. https://doi.org/10.1155/2019/3904645.
[42] Dehghan Harati M, Rodemann HP, Toulany M. Nanog Signaling Mediates Radioresistance in ALDH-Positive Breast Cancer Cells. Int J Mol Sci 2019;20. https://doi.org/10.3390/ijms20051151.
[43] Mele L, Liccardo D, Tirino V. Evaluation and Isolation of Cancer Stem Cells Using ALDH Activity Assay. Methods Mol Biol 2018;1692:43–8. https://doi.org/10.1007/978-1-4939-7401-6_4.
[44] Clark DW, Palle K. Aldehyde dehydrogenases in cancer stem cells: potential as therapeutic targets. Ann Transl Med 2016;4. https://doi.org/10.21037/atm.2016.11.82.
[45] Cui X, Oonishi K, Tsujii H, Yasuda T, Matsumoto Y, Furusawa Y, et al. Effects of Carbon Ion Beam on Putative Colon Cancer Stem Cells and Its Comparison with X-rays. Cancer Res 2011:canres.2926.2010. https://doi.org/10.1158/0008-5472.CAN-10-2926.
[46] Oonishi K, Cui X, Hirakawa H, Fujimori A, Kamijo T, Yamada S, et al. Different effects of carbon ion beams and X-rays on clonogenic survival and DNA repair in human pancreatic cancer stem-like cells. Radiotherapy and Oncology 2012;105:258–65. https://doi.org/10.1016/j.radonc.2012.08.009.
[47] Pattabiraman DR, Weinberg RA. Tackling the cancer stem cells – what challenges do they pose? Nat Rev Drug Discov 2014;13:497–512. https://doi.org/10.1038/nrd4253.
[48] Takahashi R, Miyazaki H, Ochiya T. The role of microRNAs in the regulation of cancer stem cells. Front Genet 2014;4. https://doi.org/10.3389/fgene.2013.00295.
[49] Cheng C-Y, Hwang C-I, Corney DC, Flesken-Nikitin A, Jiang L, Öner GM, et al. miR-34 Cooperates with p53 in Suppression of Prostate Cancer by Joint Regulation of Stem Cell Compartment. Cell Reports 2014;6:1000–7. https://doi.org/10.1016/j.celrep.2014.02.023.
[50] Yoshitaka T, Kawai A, Miyaki S, Numoto K, Kikuta K, Ozaki T, et al. Analysis of microRNAs expressions in chondrosarcoma. Journal of Orthopaedic Research 2013;31:1992–8. https://doi.org/10.1002/jor.22457.
[51] Hermeking H. The miR-34 family in cancer and apoptosis. Cell Death and Differentiation 2010;17:193–9. https://doi.org/10.1038/cdd.2009.56.

[52]Stebbing J, Shah K, Lit LC, Gagliano T, Ditsiou A, Wang T, et al. LMTK3 confers chemo-resistance in breast cancer. Oncogene 2018;37:3113–30. https://doi.org/10.1038/s41388-018-0197-0.
[53]Venkatesh V, Nataraj R, Thangaraj GS, Karthikeyan M, Gnanasekaran A, Kaginelli SB, et al. Targeting Notch signalling pathway of cancer stem cells. Stem Cell Investig 2018;5. https://doi.org/10.21037/sci.2018.02.02.
[54]Qi X, Li Y, Zhang Y, Xu T, Lu B, Fang L, et al. KLF4 functions as an oncogene in promoting cancer stem cell-like characteristics in osteosarcoma cells. Acta Pharmacol Sin 2019;40:546–55. https://doi.org/10.1038/s41401-018-0050-6.
[55]Zhang H-L, Wang P, Lu M-Z, Zhang S-D, Zheng L. c-Myc maintains the self-renewal and chemoresistance properties of colon cancer stem cells. Oncol Lett 2019;17:4487–93. https://doi.org/10.3892/ol.2019.10081.
[56]Yu M, Hao B, Zhan Y, Luo G. Krüppel-like factor 4 expression in solid tumor prognosis: A meta-analysis. Clinica Chimica Acta 2018;485:50–9. https://doi.org/10.1016/j.cca.2018.06.030.
[57]Zhang L, Zhang L, Xia X, He S, He H, Zhao W. Krüppel-like factor 4 promotes human osteosarcoma growth and metastasis via regulating CRYAB expression. Oncotarget 2016;7:30990–1000. https://doi.org/10.18632/oncotarget.8824.
[58]Cittelly DM, Finlay-Schultz J, Howe EN, Spoelstra NS, Axlund SD, Hendricks P, et al. Progestin suppression of miR-29 potentiates dedifferentiation of breast cancer cells via KLF4. Oncogene 2013;32:2555–64. https://doi.org/10.1038/onc.2012.275.
[59]Kang L, Mao J, Tao Y, Song B, Ma W, Lu Y, et al. MicroRNA-34a suppresses the breast cancer stem cell-like characteristics by downregulating Notch1 pathway. Cancer Science 2015;106:700–8. https://doi.org/10.1111/cas.12656.
[60]Pramanik D, Campbell NR, Karikari C, Chivukula R, Kent OA, Mendell JT, et al. Restitution of tumor suppressor microRNAs using a systemic nanovector inhibits pancreatic cancer growth in mice. Mol Cancer Ther 2011;10:1470–80. https://doi.org/10.1158/1535-7163.MCT-11-0152.
[61]Nwani NG, Condello S, Wang Y, Swetzig WM, Barber E, Hurley T, et al. A Novel ALDH1A1 Inhibitor Targets Cells with Stem Cell Characteristics in Ovarian Cancer. Cancers 2019;11:502. https://doi.org/10.3390/cancers11040502.
[62]Yadav RK, Chauhan AS, Zhuang L, Gan B. FoxO transcription factors in cancer metabolism. Seminars in Cancer Biology 2018;50:65–76. https://doi.org/10.1016/j.semcancer.2018.01.004.
[63]Chen C-C, Jeon S-M, Bhaskar PT, Nogueira V, Sundararajan D, Tonic I, et al. FoxOs inhibit mTORC1 and activate Akt by inducing the expression of Sestrin3 and Rictor. Dev Cell 2010;18:592–604. https://doi.org/10.1016/j.devcel.2010.03.008.
[64]Mori S, Nada S, Kimura H, Tajima S, Takahashi Y, Kitamura A, et al. The mTOR Pathway Controls Cell Proliferation by Regulating the FoxO3a Transcription Factor via SGK1 Kinase. PLOS ONE 2014;9:e88891. https://doi.org/10.1371/journal.pone.0088891.
[65]Natarajan SK, Stringham BA, Mohr AM, Wehrkamp CJ, Lu S, Phillippi MA, et al. FoxO3 increases miR-34a to cause palmitate-induced cholangiocyte lipoapoptosis. J Lipid Res 2017;58:866–75. https://doi.org/10.1194/jlr.M071357.
[66]Liu X, Feng J, Tang L, Liao L, Xu Q, Zhu S. The regulation and function of miR-21-FOXO3a-miR-34b/c signaling in breast cancer. Int J Mol Sci 2015;16:3148–62. https://doi.org/10.3390/ijms16023148.
[67]Ames E, Canter RJ, Grossenbacher SK, Mac S, Smith RC, Monjazeb AM, et al. Enhanced targeting of stem-like solid tumor cells with radiation and natural killer cells. OncoImmunology 2015;4:e1036212. https://doi.org/10.1080/2162402X.2015.1036212.
[68]Diaz R, Nguewa PA, Redrado M, Manrique I, Calvo A. Sunitinib reduces tumor hypoxia and angiogenesis, and radiosensitizes prostate cancer stem-like cells. The Prostate 2015;75:1137–49. https://doi.org/10.1002/pros.22980.

Figure legends

Figure 1. CH-2879 chondrosarcoma cells contain a radioresistant cancer stem cell subpopulation suppressed by miR-34. **a** Sorting of ALDH+ cancer stem cells. DEAB-treated cells served as negative control. The proportion of ALDH+ cells was measured after carbon-ion irradiation and/or treatment with miR-34 mimic (34m), rapamycin (rap) or rapamycin + FOXO3 siRNA (rap+Fsi). **b,c,d** Invasion scratch assay (**b)**, sphere-formation assay (**c**) and reactive oxygen species (ROS) level measurements (**d**) were performed in ALDH- and ALDH+ cells after treatment with miR-34 mimic (34m). **e** Dose-response curves for clonogenic survival of CH-2879 chondrosarcoma cells. ALDH- and ALDH+ cells were exposed to X-rays or carbon-ion beam (the differences of clonogenic survival between ALDH- and ALDH+ cells were significant for every dose after X-ray irradiation and after 2-5 Gy carbon-ion). Results are expressed as the mean ± SD of three or more independent experiments.

Figure 2. miR34 exerts its effects via KLF4 and protects against tumor formation. **a,b** Expression of miR-34 (**a**) and miR-34 target genes (**b**) in ALDH+ cells, relative to ALDH- cells. **c** KLF4 protein expression levels in ALDH- and ALDH+ cells after treatment with miR-34 mimic (34m) or transfection with FOXO3 expression vector (fox). **d** Sphere formation assay in ALDH+ cells after treatment with KLF4 siRNA. Results are expressed as the mean ± SD of three or more independent experiments. **e,f** Growth of chondrosarcoma subcutenous xenografts (**e**) was measured by external caliper in nude mice, after injection of ALDH- or ALDH+ cells and/or miR-34 administration (**f**). Results are expressed as the mean ± SD for five or more animals.

Figure 3. mTOR inhibition by Rapamycin targets chondrosarcoma stem cells via FOXO3 and miR-34. **a,b** Expression of miR-34 (**a**) and miR-34 target genes (**b**) after rapamycin treatment, relative to non-treated cells. **c** FOXO3 promoter activity after transfection with FOXO expression vector or rapamycin treatment. **d** Sphere formation assay in ALDH+ cells after treatment with FOXO expression vector (FOXO3), rapamycin (rap) or rapamycin + FOXO3 siRNA (Fsi). **e,f** Expression of miR-34 (**e)**

and miR-34 target genes (**f**) in cells transfected with FOXO expression vector, relative to cells treated with control vector. Results are expressed as the mean ± SD of three or more independent experiments.

Figure 4. a Sphere formation assay after treatment with miR-34 mimic and/or rapamycin, when cells where plated at various times following treatment. **b** Proportion of remaining ALDH+ CSCs after exposure to 1 Gy carbon-ion, equivalent dose 2 Gy X-rays in cells treated with rapamycin alone or in combination with miR-34 mimic, relative to the proportion of ALDH+ cells in non-irradiated, untreated cells. Results are expressed as the mean ± SD of three or more independent experiments.

Annex A. Supplementary data

Supplementary data available.

Table A1. Chondrosarcoma cell lines.

Table A2. Primers for quantitative real-time PCR.

Table A3. TCGA survival Cox regression results for miR-34 and for 18 miR-34 target genes in sarcoma patients.

Figure A1. Transcriptional response of CH-2879 cells to carbon-ion irradiation (a) Number of deregulated genes 24h after exposure to various irradiation doses (b) Multi-dimensional scaling (MDS) plot showing sample relations. (c) Top Regulator Effect Networks in Ingenuity Pathway Analysis (IPA). p53-associated networks are highlighted in pink.

Figure A2. Apoptosis of CH-2879 cells after miR-34 mimic administration.

Figure A3. Electropherograms for KLF4 and GAPDH expression.

Figure A4. CH-2879 cell proliferation after rapamycin treatment.

Figure A5. Dose-response curves for clonogenic survival of CH-2879 cells after rapamycin treatment and carbon-ion irradiation.

Figure A6. Kaplan-Meier survival curves of sarcoma patients with high (top third) or low (bottom third) expression.

		D10	D37	SF2	$RBE_{(D10)}$	$RBE_{(D37)}$
X-rays	ALDH-	2.97	1.29	0.21		
	ALDH+	3.64	1.62	0.29		
Carbon-ion	ALDH-	1.57	0.68	0.05	1.89	1.90
	ALDH+	1.96	0.84	0.09	1.86	1.93

Table 1: Clonogenic survival characteristics of CH-2879 cells exposed to X-rays or Carbon-ion beam.

Injection	Control	miR-34 mimic
1,000 ALDH-	0/4 (0 %)	0/4 (0 %)
1,000 ALDH+	0/4 (0 %)	0/4 (0 %)
10,000 ALDH-	0/4 (0 %)	0/4 (0 %)
10,000 ALDH+	5/5 (100 %)	1/5 (20 %)
100,000 ALDH-	1/5 (20%)	0/5 (0 %)
100,000 ALDH+	9/9 (100%)	4/9 (45 %)

Table 2. Induction of xenograft tumors in nude mice after administration of increasing numbers of CH-2879 cells and miR-34 mimic.

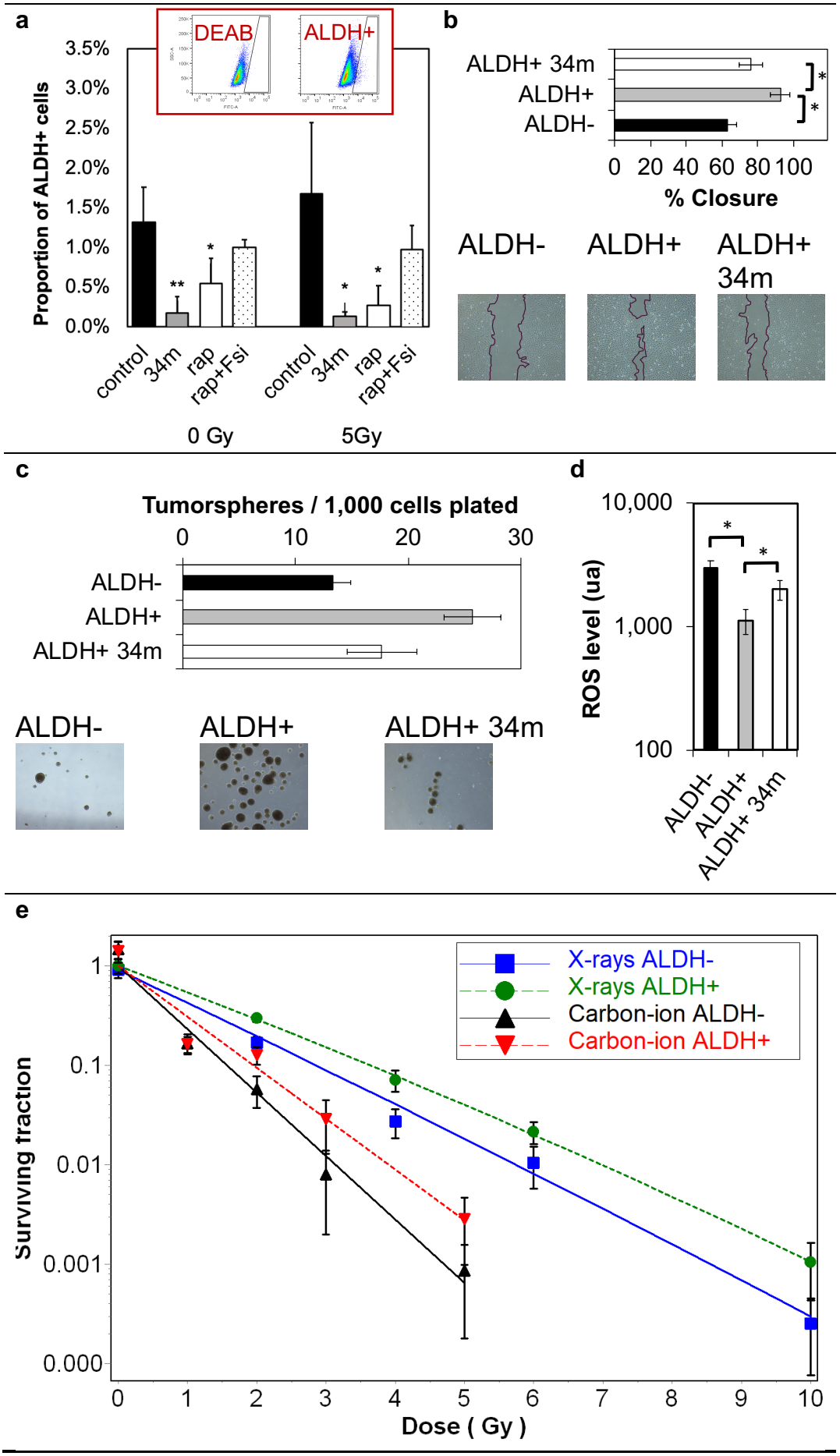
a
DEAB
ALDH+
Proportion of ALDH+ cells
3.5%
3.0%
2.5%
2.0%
1.5%
1.0%
0.5%
0.0%
control
34m
rap
rap+Fsi
0 Gy
5Gy
b
ALDH+ 34m
ALDH+
ALDH-
0 20 40 60 80 100
% Closure
ALDH-
ALDH+
ALDH+ 34m
c
Tumorspheres / 1,000 cells plated
0
10
20
30
ALDH-
ALDH+
ALDH+ 34m
d
ROS level (ua)
10,000
1,000
100
ALDH-
ALDH+
ALDH+ 34m
e
Surviving fraction
1
0.1
0.01
0.001
0.000
0 1 2 3 4 5 6 7 8 9 10
Dose (Gy)
X-rays ALDH-
X-rays ALDH+
Carbon-ion ALDH-
Carbon-ion ALDH+

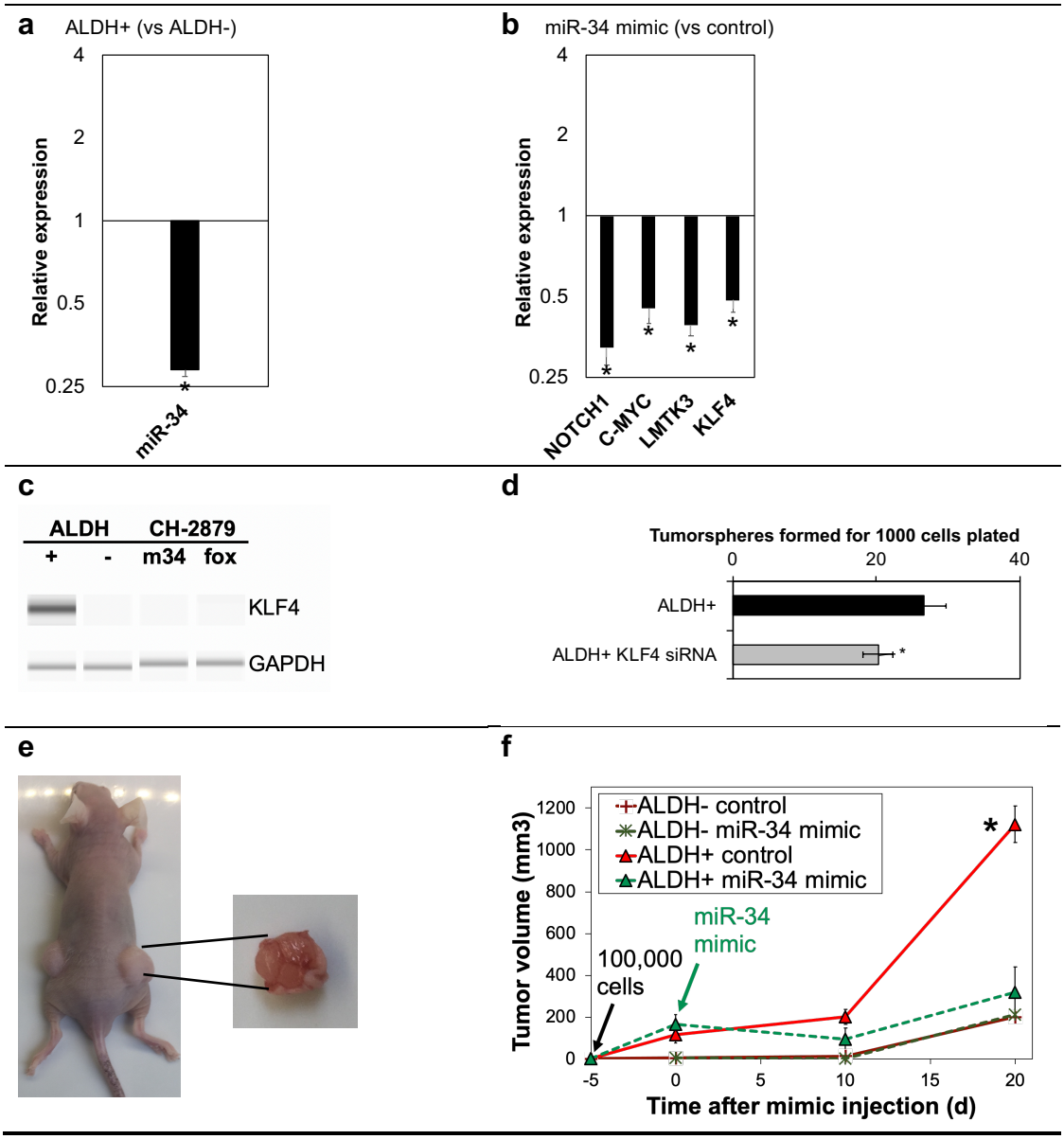
a
ALDH+ (vs ALDH-)
Relative expression
4
2
1
0.5
0.25
*
miR-34
b
miR-34 mimic (vs control)
Relative expression
4
2
1
0.5
0.25
*
*
*
*
NOTCH1
C-MYC
LMTK3
KLF4
c
ALDH
CH-2879
+
-
m34
fox
KLF4
GAPDH
d
Tumorspheres formed for 1000 cells plated
0
20
40
ALDH+
ALDH+ KLF4 siRNA
*
e
f
ALDH- control
ALDH- miR-34 mimic
ALDH+ control
ALDH+ miR-34 mimic
Tumor volume (mm3)
1200
1000
800
600
400
200
0
miR-34
mimic
100,000
cells
*
-5
0
5
10
15
20
Time after mimic injection (d)

Figure 2

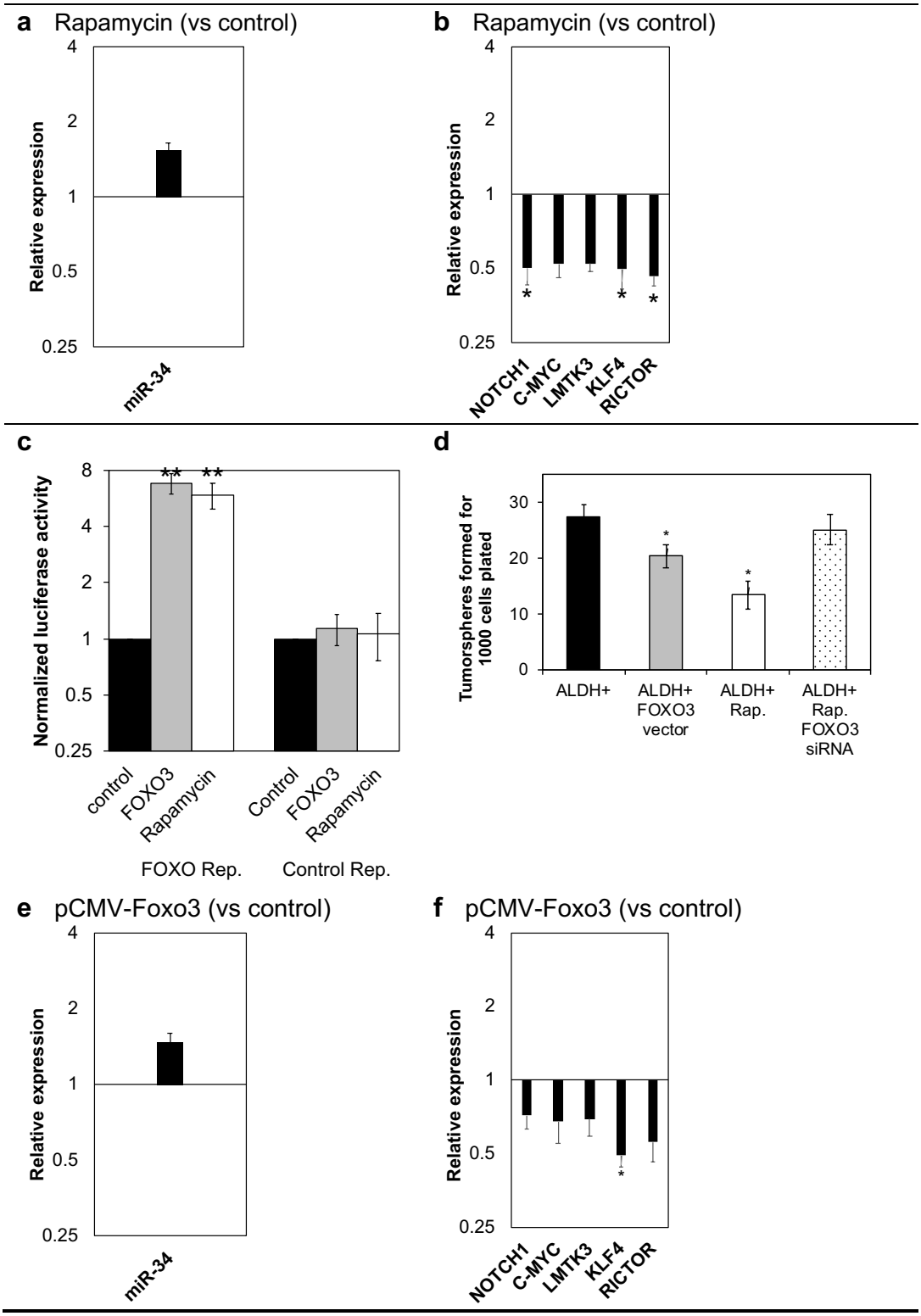
a Rapamycin (vs control)
Relative expression
4
2
1
0.5
0.25
miR-34
b Rapamycin (vs control)
Relative expression
4
2
1
0.5
0.25
*
*
*
NOTCH1
C-MYC
LMTK3
KLF4
RICTOR
c
Normalized luciferase activity
8
4
2
1
0.5
0.25
**
**
control
FOXO3
Rapamycin
Control
FOXO3
Rapamycin
FOXO Rep.
Control Rep.
d
Tumorspheres formed for 1000 cells plated
30
20
10
0
*
*
ALDH+
ALDH+ FOXO3 vector
ALDH+ Rap.
ALDH+ Rap. FOXO3 siRNA
e pCMV-Foxo3 (vs control)
Relative expression
4
2
1
0.5
0.25
miR-34
f pCMV-Foxo3 (vs control)
Relative expression
4
2
1
0.5
0.25
*
NOTCH1
C-MYC
LMTK3
KLF4
RICTOR

Figure 3

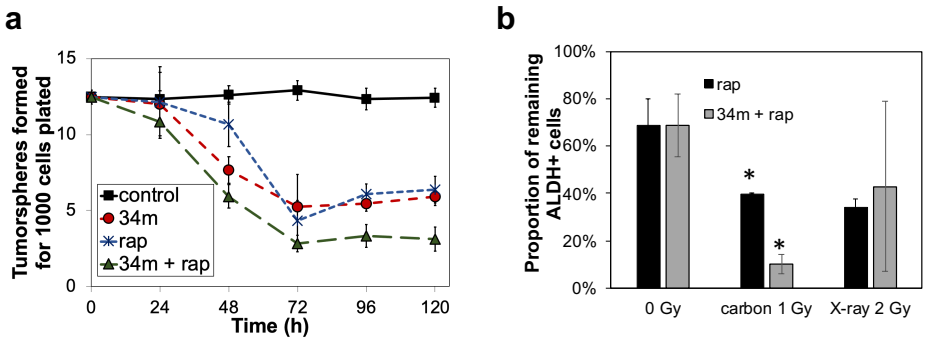
a
Tumorspheres formed for 1000 cells plated
15
10
5
0
0
24
48
72
96
120
Time (h)
control
34m
rap
34m + rap
b
Proportion of remaining ALDH+ cells
100%
80%
60%
40%
20%
0%
rap
34m + rap
*
*
0 Gy
carbon 1 Gy
X-ray 2 Gy

Figure 4

Appendix A. Supplementary Information

A multimodal treatment of carbon ions irradiation, miRNA-34 and mTOR inhibitor specifically control high-grade chondrosarcoma cancer stem cells

Guillaume Vares[a], Vidhula Ahire[b, c], Shigeaki Sunada[d,e], Eun Ho Kim[f], Sei Sai[g], François Chevalier[b, c], Paul-Henri Romeo[h], Tadashi Yamamoto[a], Tetsuo Nakajima[d] and Yannick Saintigny[b, c]

[a] Cell Signal Unit, Okinawa Institute of Science and Technology Graduate University (OIST), Tancha 1919-1, Onna-son, Okinawa, Japan
[b] Research Laboratory and Open Facility for Radiation Biology with Accelerated Ions (LARIA), CEA/DRF/IBFJ/IRCM, Campus Jules Horowitz, Boulevard Henri Becquerel, Caen, France
[c] Centre de Recherche sur les Ions, les Matériaux et la Photonique (CIMAP), Normandie Univ/ ENSICAEN/UNICAEN/CEA/CNRS, Campus Jules Horowitz, Boulevard Henri Becquerel, Caen, France
[d] Department of Radiation Effects Research, National Institutes for Quantum and Radiological Science and Technology (QST), Anagawa 4-9-1, Inage-ku, Chiba, Japan
[e] Department of Molecular Genetics, Tokyo Medical and Dental University (TMDU), 1-5-45 Yushima, Bunkyo-ku, Tokyo, Japan
[f] Division of Radiation Biomedical Research, Korea Institute of Radiological and Medical Sciences (KIRAMS), 75 Nowon-ro, Gongneung 2(i)-dong, Nowon-gu, Seoul, South Korea
[g] Department of Charged Particle Therapy Research, National Institutes for Quantum and Radiological Science and Technology (QST), Anagawa 4-9-1, Inage-ku, Chiba, Japan
[h] Research Laboratory on repair and Transcription in hematopoietic Stem Cells (LRTS), François Jacob Institute of biology, CEA/DRF/IBFJ/IRCM, 18 Route du Panorama, Fontenay-aux-Roses, France

Name	Diagnosis	Grade	Reference
CH-2879	Chondrosarcoma	III	[1]
OUMS27	Chondrosarcoma	III	[2]
L835	Chondrosarcoma	III	[3]
SW-1353	Chondrosarcoma	II	[4]

Table A1: Chondrosarcoma cell lines.

Gene	Forward	Reverse
NOTCH1	CTGAAGAACGGGGCTAACAA	AGTGGTCCAGCAGCACCTT
C-MYC	CCACACATCAGCACAACTACGC	CGGTTGTTGCTGATCTGTCTCA
LMTK3	TCGGCTTCAAGGAATTTGAGA	GGGTGGTCATGTCTGAGTGTGA
KLF4	GCCCCTCGGGCGGCTTCGTGGCCGAGCTC	CGTACTCGCTGCCAGGGGCG
RICTOR	CCGTGTCGGAGGTTCATACA	GCCTCTGCTTCTTCATGCATT
GAPDH	GAAGGTGAAGGTCGGAGTCA	TTGATGGCAACAATATCCACTT

Table A2: Primers for quantitative real-time PCR.

a

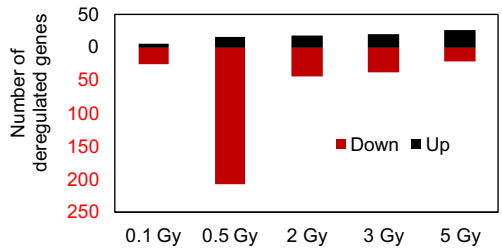

b

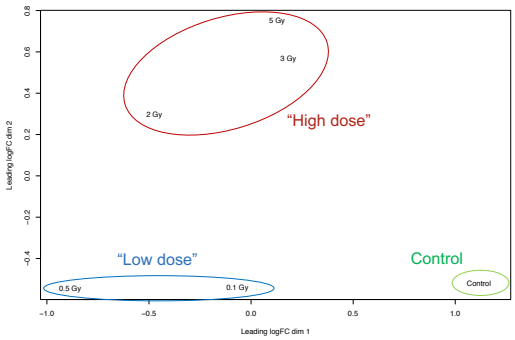

c

	0.2 Gy	0.5 Gy	2 Gy	3 Gy	5 Gy
1	CA4, miR-1254	IL19, ITIH1, NR4A	miR-1225	CYR61, EGF	miR-6825
					Death
2	miR-593	miR-1343	miR-1225	Ap1, APOE, HDAC2	miR-3104
				Proliferation	**Death**
3	CASP8, miR-4781	Gsk3, miR-3605	CSF2	CYR61	miR-3175
	Communication				**Death**
4	SMARCA4	miR-185	miR-193	miR-1268a	miR-6795
		Proliferation			**Death**
5	miR-1283h	CD24, FZD8	CDKN2A	ABCB4, FZD8	miR-149
				Metastasis	**Death**

p53-associated

Figure A1: Transcriptional response of CH-2879 cells to carbon-ion irradiation (a) Number of deregulated genes 24h after exposure to various irradiation doses (b) Multi-dimensional scaling (MDS) plot showing sample relations. (c) Top Regulator Effect Networks in Ingenuity Pathway Analysis (IPA). p53-associated networks are highlighted in pink.

Using RNA-Seq, we measured gene regulations in CH-2879 cells one day after carbon-ion exposure. A number of genes were up- or down-regulated (Figure A1a), and multi-dimensional scaling (MDS) analysis supported the partition of irradiation doses into two groups ("low doses" and "high doses"). The investigation of individual gene deregulations as well as the determination of regulator effect networks suggested that only high doses (in particular the highest dose of 5 Gy) predominantly activated stress response pathways and cell death-associated mechanisms.

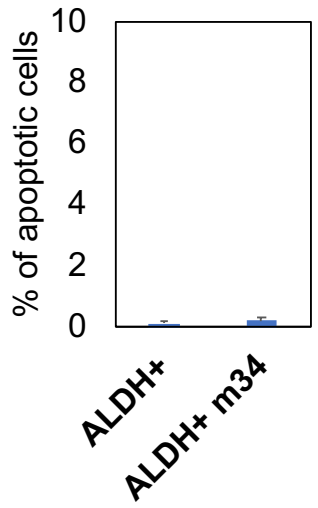

Figure A2: Apoptosis of CH-2879 cells after miR-34 mimic administration.

	KLF4	GAPDH
ALDH+ control	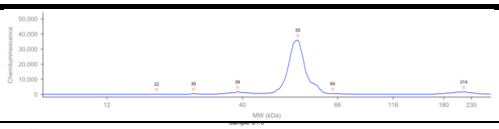	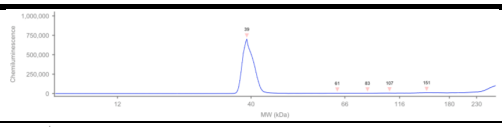
ALDH- Control	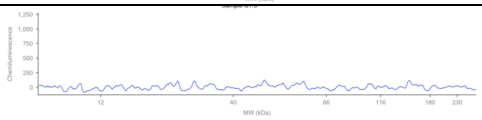	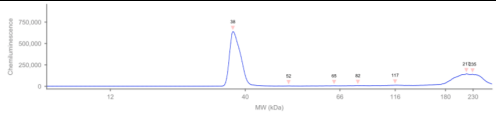
ALDH+ m34	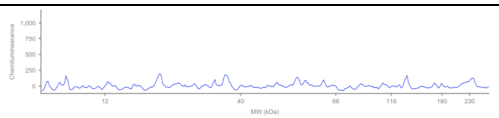	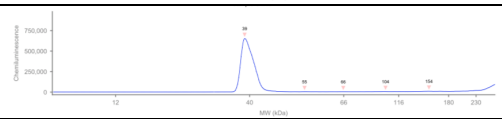
ALDH+ fox	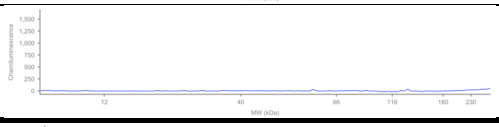	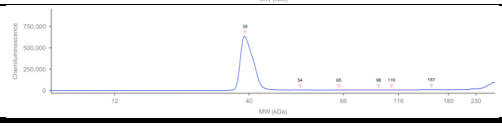
Ladder	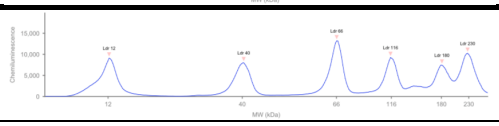	

Figure A3: Electropherograms for KLF4 and GAPDH expression after in ALDH- and ALDH+ cells after treatment with miR-34 mimic (34m) or transfection with FOXO3 expression vector (fox).

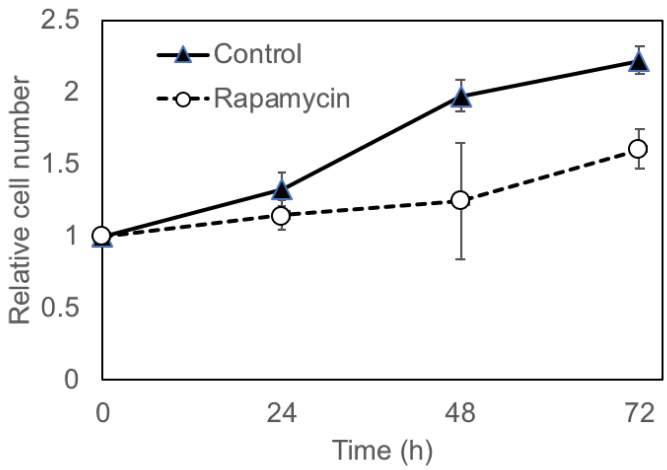

Figure A4: CH-2879 cell proliferation after rapamycin treatment.

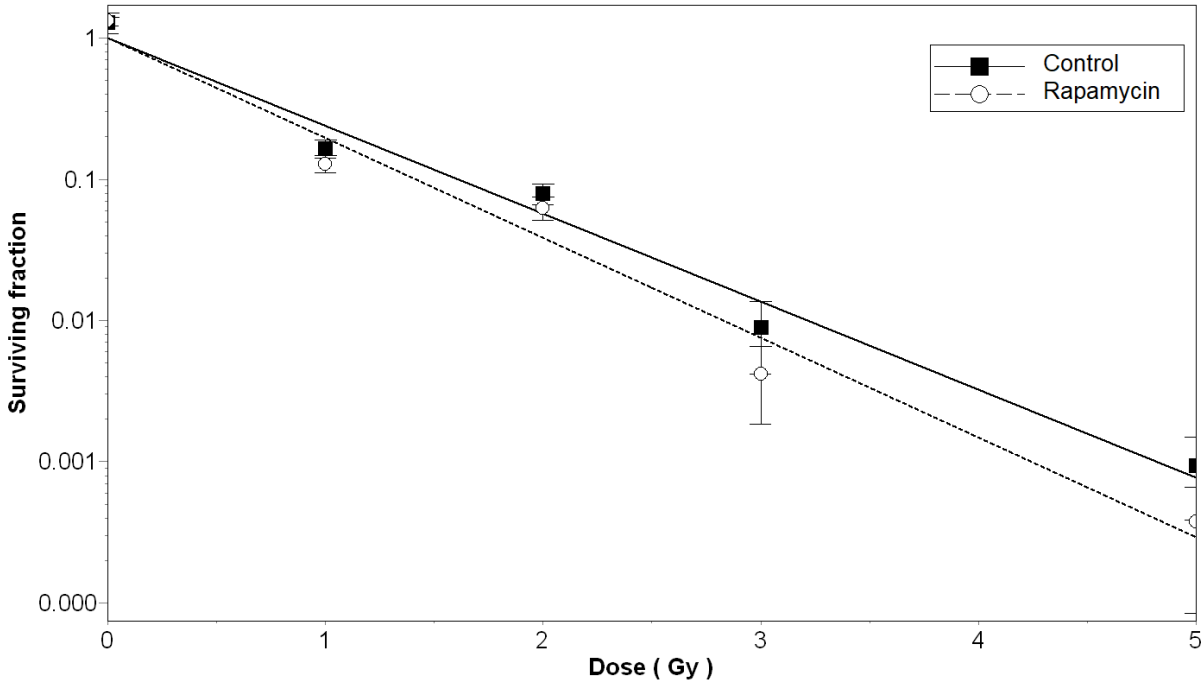

Figure A5: Dose-response curves for clonogenic survival of CH-2879 cells after rapamycin treatment and carbon-ion irradiation.

Transcript	Cox Coefficient	P-Value	FDR Corrected	Rank
hsa-MIR-34A-5P	0.069	0.51	0.622	373
NOTCH1	-0.117	0.27	0.565	7716
C-MYC	0.265	0.012	0.113	1703
LMTK3	0.027	0.8	0.915	14126
KLF4	-0.103	0.31	0.605	8240
RICTOR	-0.114	0.29	0.586	8008
BCL2	0.097	0.37	0.654	9054
CCND1	-0.04	0.69	0.863	12876
CCNE2	0.121	0.24	0.532	7204
CDK4	0.213	0.033	0.191	2764
CDK6	0.144	0.18	0.460	6195
E2F3	0.395	1.80×10^{-4}	0.0146	197
HDAC1	0.237	0.034	0.193	2825
JAG1	-0.152	0.11	0.352	4947
MDM4	0.004	0.97	0.987	15907
MET	0.101	0.35	0.639	8819
NOTCH2	-0.02	0.86	0.944	14748
SIRT1	0.083	0.43	0.701	9934
WNT1	-0.053	0.62	0.826	12179

Table A3: TCGA survival Cox regression results for miR-34 and for 18 miR-34 target genes in sarcoma patients.

Transcript	Logrank p-Value	
hsa-MIR-34A-5P	0.742	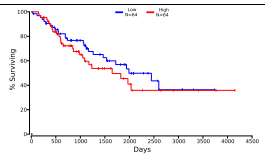
NOTCH1	0.0373	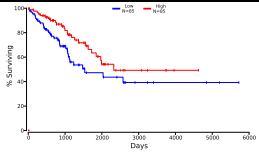
C-MYC	0.0078	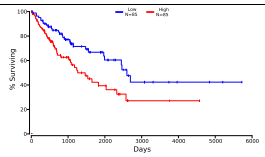
LMTK3	0.341	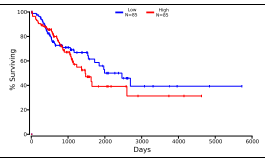
KLF4	0.416	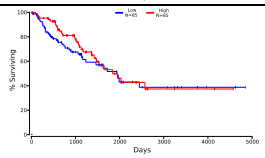
RICTOR	0.454	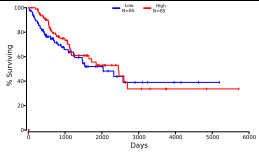
BCL2	0.721	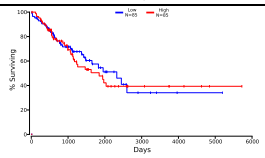
CCND1	0.627	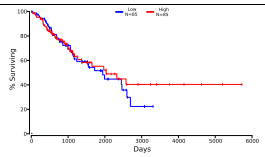
CCNE2	0.0558	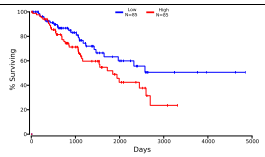
CDK4	0.00961	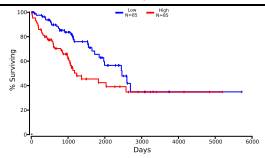
CDK6	0.0115	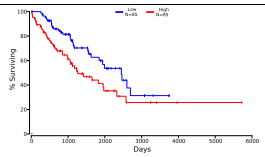

E2F3	3.79e-05	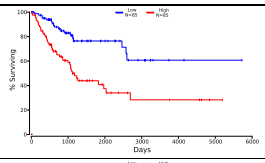
HDAC1	0.147	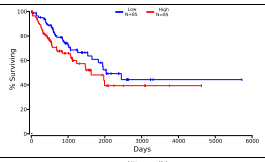
JAG1	0.379	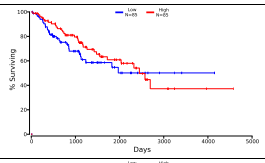
MDM4	0.384	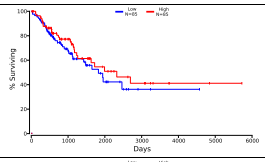
C-MET	0.16	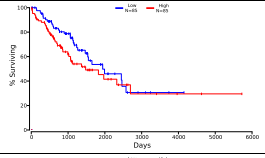
NOTCH2	0.277	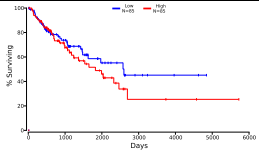
SIRT1	0.272	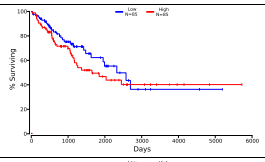
WNT1	0.994	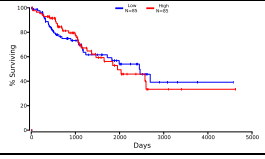

Figure A6: Kaplan-Meier survival curves of sarcoma patients with high (top third) or low (bottom third) expression.

Supplementary material and methods

RNA-Seq. RNA was extracted using Trizol and a column-based PureLink RNA Mini Kit (Invitrogen, Carlsbad, CA, USA). RNA-sequence libraries were prepared with the TruSeq Stranded mRNA NeoPrep kit (Illumina, San Diego, CA, USA). Sequencing was performed on a HiSeq 4000 machine (Illumina) to generate 150 nucleotide paired-end reads at a depth of at least 40 million reads. After quality control with FastQC, reads were mapped to the hg19 reference human genome using tophat2 software (v2.1.1), assembled and quantified using the cufflinks software suite (v2.2.1)[5]. Differentially expressed genes were counted and analyzed with Ingenuity Pathway Analysis (Qiagen, Hilden, Germany)[6]. Mapped reads were also sorted with samtools (v1.3.1), read counts were then quantified with HTSeq-count (v0.9.1) and analyzed with the edgeR package (v3.22.5, using Bioconductor v3.7 on R v3.5.0) for multi-dimensional scaling (MDS)[7]. The sequencing data have been deposited in the Gene Expression Omnibus (GEO) database (Accession Number GSE135371).

Apoptosis. Cells were washed with PBS, then stained with Annexin V-FITC and PI at room temperature in the dark using Annexin V-FITC Apoptosis Detection Kit (Nacalai, Kyoto, Japan). The stained cells were analyzed with a FACSAria flow cytometer (Becton Dickinson, San Jose, CA, USA). Apoptosis was shown as the percentage of apoptotic cells to the total number of counted cells.

TCGA analysis. Data from 259 sarcoma patients downloaded from the Cancer Genome Atlas (TCGA) were used to correlate gene expression and survival, using OncoLnc tool (http://www.oncolnc.org/). For each gene, Cox regression analysis was performed then sarcoma patients were divided in high (top third) or low (bottom third) expression groups and survival of the two groups was compared using Kaplan-Meier plots and log rank analysis[8].

References

1 Gil-Benso R, Lopez-Gines C, López-Guerrero JA, Carda C, Callaghan RC, Navarro S *et al*. Establishment and Characterization of a Continuous Human Chondrosarcoma Cell Line, *ch-2879*: Comparative Histologic and Genetic Studies with Its Tumor of Origin. *Laboratory Investigation* 2003; **83**: 877–887.

2 Kunisada T, Miyazaki M, Mihara K, Gao C, Kawai A, Inoue H *et al*. A new human chondrosarcoma cell line (OUMS-27) that maintains chondrocytic differentiation. *Int J Cancer* 1998; **77**: 854–859.

3 van Oosterwijk JG, de Jong D, van Ruler MAJH, Hogendoorn PCW, Dijkstra PDS, van Rijswijk CSP *et al*. Three new chondrosarcoma cell lines: one grade III conventional central chondrosarcoma and two dedifferentiated chondrosarcomas of bone. *BMC Cancer* 2012; **12**: 375.

4 Hay RJ. Development, Availability and Characterization of ATCC Human and Animal Cell Lines. In: Sasaki R, Ikura K (eds). *Animal Cell Culture and Production of Biologicals: Proceedings of the Third Annual Meeting of the Japanese Association for Animal Cell Technology, held in Kyoto, December 11–13, 1990*. Springer Netherlands: Dordrecht, 1991, pp 27–39.

5 Differential gene and transcript expression analysis of RNA-seq experiments with TopHat and Cufflinks | Nature Protocols. https://www.nature.com/articles/nprot.2012.016.

6 Krämer A, Green J, Pollard J, Tugendreich S. Causal analysis approaches in Ingenuity Pathway Analysis. *Bioinformatics* 2014; **30**: 523–530.

7 McCarthy DJ, Chen Y, Smyth GK. Differential expression analysis of multifactor RNA-Seq experiments with respect to biological variation. *Nucleic Acids Res* 2012; **40**: 4288–4297.

8 Anaya J. OncoLnc: linking TCGA survival data to mRNAs, miRNAs, and lncRNAs. *PeerJ Comput Sci* 2016; **2**: e67.